

Adaptive Local Regularization Methods for the Inverse ECG Problem

Christopher R. Johnson¹ and Robert S. MacLeod²

¹Department of Computer Science and ²Cardiovascular Research and Training Institute
University of Utah, Salt Lake City, UT 84112
Email: crj@cs.utah.edu and macleod@cvrti.utah.edu

Abstract

One of the fundamental problems in theoretical electrocardiography can be characterized by an inverse problem. We present new methods for achieving better estimates of heart surface potential distributions in terms of torso potentials through an inverse procedure. First, we outline an automatic adaptive refinement algorithm that minimizes the spatial discretization error in the transfer matrix, increasing the accuracy of the inverse solution. Second, we introduce a new local regularization procedure, which works by partitioning the global transfer matrix into sub-matrices, allowing for varying amounts of smoothing. Each submatrix represents a region within the underlying geometric model in which regularization can be specifically ‘tuned’ using an *a priori* scheme based on the L-curve method. This *local* regularization method can provide a substantial increase in accuracy compared to global regularization schemes. Within this context of local regularization, we show that a generalized version of the singular value decomposition (GSVD) can further improve the accuracy of ECG inverse solutions compared to standard SVD and Tikhonov approaches. We conclude with specific examples of these techniques using geometric models of the human thorax derived from MRI data.

Introduction

The intrinsic electrical activity of the heart gives rise to electric, and thus potential, fields within the volume of the thorax and upon the torso surface.

The fundamental origin of these fields arise from individual cardiac cells receiving electric current from neighboring cells and responding with a local membrane action potential. These cells then inject excitatory current into those neighboring cardiac cells that are not yet excited. High conductivity junctions exist between cardiac cells and provide the intracellular pathway for excitatory currents from activated cells to resting neighbors. An extracellular space provides the return pathway. Viewing a single time instant during the 50–100 ms required for the spread of excitation, the heart can be macroscopically represented as consisting of two regions; one containing already excited cells and the other containing cells still at rest. These two regions are separated by a complex boundary layer of approximately 1 mm thickness, across which, a large (40-80 mV) potential difference occurs. It is this macroscopic distribution of current sources (excited cells) and sinks (resting cells) that forms the time-varying bioelectric source responsible for the electrocardiogram (ECG).

The goal of solving the electrocardiographic inverse problem is to describe bioelectric cardiac sources based on knowledge of the ECG and the volume conductor that surrounds the sources. The necessary elements of such a solution include a quantitative description of the source, the geometry of the volume conductor, and the equations that link source and volume conductor potentials. While a number of different source formulations are possible (see, for example ¹, for more details), the literature of the last twenty years has been dominated by two formulations that are based on the electric potentials on the surface of the heart. The first represents the entire cardiac activity by the potential distribution on a closed surface that encloses the heart; while this formulation leads to a unique inverse solution ², it is, itself, not a unique representation of underlying cardiac sources. However, if the enclosing surface corresponds to the epicardial (outer) surface of the heart, it is possible, albeit very invasive, to measure potentials on this surface and hence both validate

and interpret the results. The second formulation arises when we represent the cardiac sources as a uniform, isotropic layer of current dipoles; the layer corresponds, in simplified form, to the boundary between active and resting cells described above. The resulting electrocardiographic potentials then become simple functions of the total spatial solid angle of the excited region, which, in turn, permits a formulation of the inverse problem in terms of the boundary between excited and resting tissue over the entire epicardial and endocardial (inner) surfaces of the heart. For details of the latter formulation see ³⁻⁵. In this paper we will focus on the former approach and consider the potentials on the epicardial surface of the heart as the equivalent cardiac source.

With the source determined, our specific inverse problem is to describe potentials on the epicardial surface as a function of those on the surface of the thorax, together with knowledge of the geometric and resistive features of the intervening volume conductor. To describe these relationships mathematically, we begin with a general formulation in terms of the primary current sources within the heart described by Poisson's equation for electrical conduction:

$$\nabla \cdot \sigma \nabla \Phi = -I_v \quad \text{in } \Omega \tag{1}$$

with the boundary condition:

$$\sigma \nabla \Phi \cdot \mathbf{n} = 0 \quad \text{on } , T \tag{2}$$

where Φ are the electrostatic potentials, σ is the conductivity tensor, I_v are the cardiac current sources per unit volume, and $, T$ and Ω represent the surface and the volume of the thorax, respectively. While (1) does not have a unique solution, applying additional constraints can produce workable strategies. For example, it is possible to break up the volume of the heart into subregions, each with simplifying assumptions regarding the form of discrete sources (*e.g.*, single and multiple current dipoles, quadrupoles, *etc.*) that approximate local bioelectric sources. The goal then becomes to recover parameters such as the magnitude and direction of the simplified equivalent sources. The difficulty of this approach remains in associating these parameters with underlying physiology so that the resulting inverse solutions are useful (see ⁶⁻⁸ for a discussion of these points.)

If we now take the approach outlined above and describe the cardiac sources in terms of the

epicardial surface potentials, instead of Poisson’s equation we solve a generalized Laplace’s equation with Cauchy boundary conditions:

$$\nabla \cdot \sigma \nabla \Phi = 0 \tag{3}$$

with boundary conditions:

$$\Phi = \Phi_0 \quad \text{on } \Sigma \subseteq , T \quad \text{and} \quad \sigma \nabla \Phi \cdot \mathbf{n} = 0 \quad \text{on } , T. \tag{4}$$

Solutions to (3 and 4) can be unique and the physical quantities involved are all measurable. However, they share a characteristic of all electrocardiographic inverse problems in that they are ill-posed in the Hadamard sense; *i.e.*, because the solution does not depend continuously on the data, small errors in the measurement of the torso potentials or thorax geometry can yield unbounded errors in the solution. The origins of this ill-posedness are biophysical and lie in the attenuation of potentials as we move away from the source and the fact that the potential at any point on the torso surface is a weighted superposition of all the individual sources within the heart. Hence, the ECG represents an integration of many sources, the influence of each of which decreases sharply with distance. To solve the inverse solution, we must perform the complementary operations of amplification and differentiation on the ECG, but also on the inevitable noise that accompanies it. The result is exquisite sensitivity to any fluctuations in the input signals or geometric models.

Dealing with the ill-posed nature of the inverse problem has become the primary goal of a great deal of recent research in inverse problems as it remains the single largest obstacle to medical implementation. The most common approach is to apply constraints to the inverse solution in order to reduce its dependence on boundary conditions. The points of difficulty lie in the choice of constraints and the corresponding weight each receives in determining the best—in whatever sense we wish to define “best”—solution. Examples of recent specific approaches include constraints that change in time ⁹, constraints that change in space ^{10–12}, multiple simultaneous constraints ^{13,14}, and methods by which to determine best constraint weighting from the available *a priori* information ^{15,16} (see ¹⁷ for a recent review).

In this paper, we describe some recent progress in two facets of the inverse problem. The first

deals with improvements in the numerical techniques required to solve both the electrocardiographic forward and inverse problems when using realistic geometries. By this technique, we adjust the spatial resolution of the discrete geometry mesh in a way that reflects the estimated local error in the forward or inverse problem. The second aspect of the inverse problem we address is a form of applying constraints to the ill-conditioned discrete inverse problem to “regularize” the solution and restore continuity of the solution back onto the data. Our specific contribution lies in varying the degree of regularization constraint according to the degree of *local* ill-posedness. We show how application of these technique to a two-dimensional inverse problem can achieve noteworthy improvements in solution accuracy.

A major motivation for solving the inverse problem in electrocardiography lies in its immense clinical utility for the diagnosis and treatment of some of our most frequent and lethal health conditions. Accurate inverse solutions would improve the non-invasive evaluation of myocardial ischemia and infarcts ¹⁸, the localization of ventricular arrhythmias ¹⁹ and the site of accessory pathways in Wolff-Parkinson-White (WPW) syndrome ²⁰, and, more generally, the determination of patterns of the spread of excitation and repolarization in the heart.

Mathematical Theory

Finite Element Approximation

In order to solve the boundary value problem in (1) or (3) in terms of the epicardial potentials, we need to pose the problem in a computationally tractable way. This involves approximating the boundary value problem on a finite dimensional subspace and reformulating it in terms of a linear matrix equation—finding the forward solution that corresponds to the specific inverse problem we wish to solve . For this study we utilized the finite element method (FEM) to approximate the field equation and construct the set of matrix equations, the solution to which is a transform matrix that is the forward solution. Briefly, one starts with the Galerkin formulation of (1). Note that this includes the Dirichlet and Neumann boundary conditions,

$$(\sigma \nabla \Phi, \nabla \bar{\Phi}) = -(I_v, \bar{\Phi}), \tag{5}$$

where $\bar{\Phi}$ is an arbitrary test function, which can be thought of physically as a virtual potential field, and the notation $(\phi_1, \phi_2) \equiv \int_{\Omega} \phi_1 \phi_2 \, d\Omega$ denotes the inner product in $L_2(\Omega)$. We now use the finite element method to turn the continuous problem into a discrete formulation. First we discretize the solution domain, $\Omega = \bigcup_{e=1}^N \Omega_e$, and define a finite dimensional subspace, $V_h \subset V = \{\bar{\Phi} : \bar{\Phi} \text{ is continuous on } \Omega, \nabla \bar{\Phi} \text{ is piecewise continuous on } \Omega\}$. We define parameters of the function $\bar{\Phi} \in V_h$ at node points, $\alpha_i = \bar{\Phi}(x_i), i = 1, 2, \dots, N$ and define the basis functions $\Psi_i \in V_h$ as linear piecewise continuous functions that take the value 1 at node points and 0 elsewhere. We can then represent the function, $\bar{\Phi} \in V_h$ as:

$$\bar{\Phi} = \sum_{i=1}^N \alpha_i \Psi_i(x_i) \quad (6)$$

such that $\bar{\Phi} \in V_h$ can be written in a unique way as a linear combination of the basis functions $\Psi_i \in V_h$. The finite element approximation of the original boundary value problem (1) can be stated as:

$$\text{Find } \Phi_h \in V_h \text{ such that } (\sigma \nabla \Phi_h, \nabla \bar{\Phi}) = -(I_v, \bar{\Phi}). \quad (7)$$

Furthermore, since $\Phi_h \in V_h$ satisfies (7), then we have $(\sigma \nabla \Phi_h, \nabla \Psi) = -(I_v, \Psi_i)$. Finally, since Φ_h itself can be expressed as the linear combination:

$$\Phi_h = \sum_{i=1}^N \xi_i \Psi_i(x) \quad \xi_i = \Phi_h(x_i), \quad (8)$$

we can then write (7) as:

$$\sum_{i=1}^N \xi_i (\sigma_{ij} \nabla \Psi_i, \nabla \Psi_j) = -(I_v, \Psi_j) \quad j = 1, \dots, N. \quad (9)$$

The finite element approximation of (1) can equivalently be expressed as a system of N equations with N unknowns, ξ_1, \dots, ξ_N (the electrostatic potentials). In matrix form, the above system is expressed as $A\xi = b$, where $A = (a_{ij})$ is the global stiffness matrix and has elements $(a_{ij} = (\sigma_{ij} \nabla \Psi_i, \nabla \Psi_j))$, while $b_i = -(I_v, \Psi_i)$ is the vector of source contributions. Background information on finite element methods can be found in ²¹⁻²⁴

Adaptive Methods

Solving either Poisson's or Laplace's equation by any of the standard methods (finite element, boundary element, or finite difference) for realistic shapes requires the use of discrete geometric models. Both the lack of clear relationships between level of discretization and solution accuracy as well as the large computational and manual cost of creating geometric models has lead many researchers to select approximately constant sized elements throughout the geometric models. The size and configuration of these elements also usually remain constant not only over space, but also over time, independent of any changes in the cardiac potentials.

We have found, however, that by using *a posteriori* estimates from the finite element approximation of the governing equations, along with a minimax theorem to determine the stopping criterion, we can locally refine the discretization and reduce the errors in the forward solution. It has always been assumed—and our findings support this notion—that improving the accuracy of the forward solution also improves the subsequent inverse solution. The novel aspect of our approach is that it uses local approximations of the error in the numerical solutions to drive an automatic adaptive mesh refinement ^{25,26}.

Mathematically, we can obtain an error estimator by starting from the *weak formulation* of the finite element approximation, (7). We can prove that $\Phi_h \in V_h$ (where Φ_h is the finite element solution and related to ξ by (8)) is the best approximation of the exact solution Φ in the sense that

$$\|\nabla\Phi - \nabla\Phi_h\| \leq \|\nabla\Phi - \nabla\tilde{\Phi}\| \quad \forall \tilde{\Phi} \in V_h \quad (10)$$

where

$$\|\nabla\tilde{\Phi}\| = \left(\int_{\Omega} \nabla\tilde{\Phi} \cdot \nabla\tilde{\Phi} \right)^{\frac{1}{2}}. \quad (11)$$

In particular, we can choose $\tilde{\Phi}$ to be the interpolant of Φ

$$\pi_h\Phi(N_i) = \Phi(N_i) \quad i = 1, \dots, M \quad \pi_h\Phi \in V_h. \quad (12)$$

This says that the error in the finite element approximation is bounded from above by the interpolation error. With certain constraints on our elements, we can prove the following, well know

relationships:

$$\|\nabla\Phi - \nabla\pi_h\Phi\| \leq Ch \quad (13)$$

and

$$\|\Phi - \pi_h\Phi\| \leq Ch^2 \quad (14)$$

where C is a positive constant that depends on the size of the second partial derivative of Φ and the smallest angle formed by the sides of the elements in V_h . These estimates show that the error in both Φ and $\nabla\Phi$ tend to zero as the discretization parameter, h , tends to zero. We can use these relationships to provide an adaptive algorithm for decreasing discretization error.

More precisely, we define the semi-norm:

$$|\tilde{\Phi}|_{H^r(\Omega)} = \left(\sum_{|\alpha|=r} \int_{\Omega} |D^\alpha \tilde{\Phi}|^2 dx \right)^{\frac{1}{2}} \quad (15)$$

where

$$D^\alpha \tilde{\Phi} = \frac{\partial^{|\alpha|} \tilde{\Phi}}{\partial x_1^{\alpha_1} \partial x_2^{\alpha_2}} \quad |\alpha| = \alpha_1 + \alpha_2 \quad (16)$$

are α -order partial derivatives and

$$H^K(\Omega) = \{\tilde{\Phi} \in L_2(\Omega) : D^\alpha \tilde{\Phi} \in L_2(\Omega), |\alpha| \leq K\} \quad (17)$$

defines the Sobolev spaces. Given these definitions, we can then obtain the error estimates analogous to those in (13) and (14) for the finite element approximation^{27,22}:

$$|\Phi - \Phi_h|_{H^1(\Omega)} \leq |\Phi - \pi_h\Phi|_{H^1(\Omega)} \leq C \left[\sum_{K \in T_h} (h_K |\Phi|_{H^2(K)})^2 \right]^{\frac{1}{2}} \quad (18)$$

or, in the $L_2(\Omega)$ norm,

$$\|\Phi - \Phi_h\|_{L_2(\Omega)} \leq \|\Phi - \pi_h\Phi\|_{L_2(\Omega)} \leq Ch^2 |\Phi|_{H^2(\Omega)}. \quad (19)$$

For the potential gradients we have²⁸:

$$\|\nabla\Phi - \nabla\Phi_h\|_{L_\infty(\Omega)} \leq C \|\nabla\Phi - \nabla\pi_h\tilde{\Phi}\|_{L_\infty(\Omega)} \leq C \max[h_K \max_{\alpha=2} \|D^\alpha \Phi\|_{L_\infty(\Omega)}]. \quad (20)$$

Given these previous error estimates for the finite element approximation, we can now use the estimates to decide where in our original finite element mesh the approximation is not accurate and create a recursive, adaptive algorithm to re-discretize in the appropriate areas. Suppose we want the accuracy of our finite element approximation to be within some given tolerance, δ , of the true solution, i.e.

$$|\Phi - \Phi_h|_{H^1(\Omega)} \leq \delta. \quad (21)$$

Then, we redefine our mesh until,

$$\sum_{K \in T_h} (h_k |\Phi_h|_{H^2(K)})^2 \leq \frac{\delta^2}{C^2}. \quad (22)$$

Here the sum is over all the K elements in the tessellated geometry, T_h , and we test to see if the error is less than the *normalized* tolerance. If the value of the error estimate exceeds the tolerance, the element is ‘flagged’ for further refinement. The refinement can occur either by further subdividing the egregious element (so-called h -adaption) or by increasing the order of the basis function of the element (p -adaption), or both (hp -adaption). One should note that the $H^2(\Omega)$ norm in (22) requires the second partial derivative of the finite element approximation. As stated in (8), we have assumed a linear basis function for our fundamental element. Thus, there is no continuity of the second derivative and we must approximate it using a centered difference (or other) formula based on first derivative information.

Of significant practical importance is the choice of a reasonable tolerance, δ . Since the general location and bounds of the potential field are dictated by known physiological considerations, we can generate an initial mesh based upon simple field strength-distance arguments. To estimate an upper bound of the potential (or electric) field we can compute the field strength analytically on a cylindrical surface that encloses the actual thorax geometry. The result is an estimate of the potential field and potential gradients that we then use to produce the initial graded mesh. The goal of this calculation is to assure that the errors far from the sources are minimal. We can then refine our finite element mesh by choosing the tolerance, δ , to be some fraction of the estimated error corresponding to the elements furthest from the sources. Thus we have used a minimax principle,

minimizing the maximum error based upon initial (conservative) estimates of the potential field and potential gradients ²⁵. For those unfamiliar with adaptive methods, additional information may be found in ^{29–32}.

Regularization

Traditional schemes for solving the inverse problem, (3), have involved reformulating the linear equation, $A\xi = b$, into $\xi_T = K\xi_E$, where ξ_T and ξ_E are the voltages on the body surface (torso) and heart’s surface (epicardium) respectively, and K is the $T \times E$ transfer matrix of coefficients relating the measured torso voltages to the voltages measured on the heart. From this statement of the forward problem, the inverse problem can then be expressed as $\xi_E = K^{-1}\xi_T$

Unfortunately, K is ill-conditioned, and regularization techniques are necessary to restore continuity of the solution back onto the data. Most regularization schemes treat all parts of K uniformly and apply Tikhonov, singular value decomposition (SVD), or Twomey algorithms with a single regularization parameter. Briefly, one wishes to find an approximate vector, $\xi_{E\varepsilon}$, that represents a balance between the residual error $\|\xi_T - K\xi_{E\varepsilon}\|$, which is corrupted by error and the ill-posed nature of the problem, and whatever side constraints we place on the solution based on *a priori* knowledge. Rather than applying the same level of regularization to the entire matrix K , we have found that it is possible, and advantageous, to first decompose K into submatrices and then apply regularization differently to each component of the resulting expression.

The rationale for such a local approach is that the discontinuities in the inverse solution appear irregularly distributed throughout the solution domain. Tikhonov and other regularization schemes are, in effect, filters, which restore continuity by attenuating the high (spatial) frequency components of the solution. Since regularization is usually applied globally, the results can leave some regions overly damped or smoothed while others remain poorly constrained. Our idea is then to apply regularization only to regions (represented by the sub-matrices of K) that require it and to apply different amounts of regularization to different sub-matrices.

We begin by expressing $K\xi_E = \xi_T$ for the Cauchy problem in (3) as

$$\begin{pmatrix} K_{TT} & K_{TV} & K_{TE} \\ K_{VT} & K_{VV} & K_{VE} \\ K_{ET} & K_{EV} & K_{EE} \end{pmatrix} \begin{pmatrix} \xi_T \\ \xi_V \\ \xi_E \end{pmatrix} = \begin{pmatrix} 0 \\ 0 \\ 0 \end{pmatrix}. \quad (23)$$

We can then rearrange the matrix to solve directly for the epicardial voltages in terms of the measured body surface voltages,

$$\xi_E = (K_{TV}K_{VV}^{-1}K_{VE} - K_{TE})^{-1}(K_{TT} - K_{TV}K_{VV}^{-1}K_{VT})\xi_T, \quad (24)$$

where the subscripts T , V , and E stand for the nodes in the regions of the torso, the internal volume, and epicardium, respectively. Since torso and epicardial nodes are always separated by more than one element, the K_{TE} submatrix is zero, and we can then rewrite (24) as

$$\xi_E = (K_{VE}^{-1}K_{VV}K_{TV}^{-1})(K_{TT} - K_{TV}K_{VV}^{-1}K_{VT})\xi_T. \quad (25)$$

Note that we now have inverses of three sub-matrices, K_{VE} , K_{TV} , and K_{VV} , as well as several other matrix operations to perform. If one estimates the condition number, κ , of the three sub-matrices using the ratio of the maximum to minimum singular values from a SVD, one finds that the condition number varies significantly (from $\kappa \approx 200$ for K_{VV} to $\kappa \approx 1 \times 10^{16}$ for K_{VE} in the two-dimensional model described below). Thus, one can regularize each of the sub-matrices differently, even leaving some of the other sub-matrices untouched. The overall effect of this *local regularization* is more control over the regularization process.

Since the goal of the inverse problem in electrocardiography is to accurately and noninvasively (i.e., non-surgically) estimate the voltages on the epicardial surface, we need a method to choose an *a priori* optimal regularization parameter. Traditional schemes have been based on discrepancy principles³³, quasi-optimality criterion^{33,34}, and generalized cross-validation³⁵. Recently, Hansen³⁶ has extended the observations of Lawson and Hanson³⁷ and proposed a new method for choosing the regularization parameter based on an algorithm that locates the ‘‘corner’’ of a plot of the norm (or semi-norm) of the side constraint, $\|Lx_\alpha\|$, versus the norm of the corresponding residual vector, $\|Ax_\alpha - b\|$. In this way, one can evaluate the compromise between the residual error and the effect

of the side constraint on the solution. We have utilized this *L-curve* algorithm along with our local Tikhonov regularization scheme to improve the accuracy of solutions to the inverse problem.

For the global Tikhonov regularization scheme, we can estimate $\xi_{E\varepsilon}$ by minimizing a generalized form of the Tikhonov functional:

$$M^\lambda[\xi_E, \tilde{\xi}_T, \tilde{K}] = \|K\xi_E - \tilde{\xi}_T\|_{\phi_T}^2 + \lambda\|C(\xi_E - \xi'_E)\|_{\phi_E}^2 \quad \lambda > 0 \quad (26)$$

in terms of the epicardial potentials,

$$\xi_{E\varepsilon}^\lambda = [\tilde{K}^T \tilde{K} + \lambda C^T C]^{-1} [\tilde{K}^T \tilde{\xi}_T + \lambda C^T C \xi'_E] \quad (27)$$

where \tilde{K} is the approximation of the true transformation matrix, K , $\tilde{\xi}_T$ are the measured torso potential values, ξ'_E are *a priori* constraints placed on the epicardial potentials based on physiological considerations, C is a constraint matrix (either the identity matrix, a gradient operator, or a Laplacian operator), and λ is the regularization parameter. For our *local* regularization scheme, we replace the global matrix, K , by the two sub-matrices K_{VE} and K_{TV} from (25). We note that K_{VV} in (25) has a stable inverse and, thus, does not need regularizing.

Another traditional method for regularization the ill-conditioned nature of the transfer matrix is to use a truncated SVD³⁸. The singular value decomposition of a matrix A is of the form

$$A = U\Sigma V^T = \sum_{i=1}^n u_i \sigma_i v_i^T, \quad (28)$$

where $U = (u_1, \dots, u_n) \in R^{m \times n}$ and $V = (v_1, \dots, v_n) \in R^{n \times n}$ are matrices with orthonormal columns, and where the diagonal matrix, $\Sigma = \text{diag}(\sigma_1, \dots, \sigma_n)$ has non-negative diagonal elements appearing in non-decreasing order and are called the singular values of A .

Since the condition of the matrix A can be measured (in the 2-norm) in terms of the singular values

$$\text{cond}(A) \equiv \|A\|_2 \|A^{-1}\|_2 = \sigma_1 / \sigma_n \quad (29)$$

one strategy for regularization is to sum the rank-one products of the singular value expansion only to a specified cut-off value $k < n$ where the singular value become “small.” For the electrocardiographic inverse problem, $K\xi_E = \xi_T$, this produces a truncated summation estimate for

ξ_E

$$\xi_E = K^\dagger \xi_T = \sum_i^k \frac{u_i^T \xi_T}{\sigma_i} v_i \quad (30)$$

by projecting the “good” data onto the left and right singular vectors U and V . While the truncated SVD technique provides answers comparable with Tikhonov regularization with $L = I$, it does not provide optimal results ³⁸.

A related approach that has recently been applied to regularization of ill-conditioned systems is the generalized singular value decomposition (GSVD) in which the generalized singular values of (A, L) are essentially the square roots of the generalized eigenvalues of the matrix pair $(A^T A, L^T L)$ ¹⁶. The GSVD is a decomposition of A and L in the form

$$A = U \begin{pmatrix} \Sigma & 0 \\ 0 & I_{n-p} \end{pmatrix} X^{-1} \quad (31)$$

and

$$L = v(M, 0) X^{-1} \quad (32)$$

The columns of $U \in R^{m \times n}$ and $V \in R^{p \times p}$ are orthonormal, $X \in R^{n \times n}$ is nonsingular with columns that are $A^T A$ -orthogonal, and Σ and M are $p \times p$ diagonal matrices: $\Sigma = \text{diag}(\sigma_1, \dots, \sigma_p)$, $M = \text{diag}(\mu_1, \dots, \mu_p)$. The *generalized* singular values γ_i of (A, L) are defined as the ratios of σ_i and μ_i

$$\gamma_i = \frac{\sigma_i}{\mu_i} \quad (33)$$

The pseudo-inverse of A in terms of the GSVD can be computed as

$$A^\dagger = X \begin{pmatrix} \Sigma^\dagger & 0 \\ 0 & I_{n-p} \end{pmatrix} U^T \quad (34)$$

such that a regularized solution can be written as

$$\xi_E = X \Phi \begin{pmatrix} \Sigma^\dagger & 0 \\ 0 & I_{n-p} \end{pmatrix} U^T \xi_T \quad (35)$$

where Φ are called the *filter factors* and depend on the amount of regularization. In this case, one would truncate the offending singular values, as well as modify the basis of the right singular vectors with the L operator. We have found that using L operators that approximate the operator

of the original governing partial differential equation (in this case the Laplacian), provide the best results. However, constructing the “best” L operator is still a topic for further research.

Results and Discussion

To study forward and inverse problems in electrocardiography, we developed a series of two- and three-dimensional boundary element and finite element models based upon magnetic resonance images from a human subject. Each of 116 MRI scans were segmented into contours defining torso, fat, muscle, lung, and heart regions. Additional node points were added to digitize each layer and pairs of layers tessellated into tetrahedra using a Delaunay triangulation algorithm^{39,40}. The resulting model of the human thorax contained approximately 675,000 volume elements, each with a corresponding conductivity tensor⁴¹. A single (two-dimensional) layer of this model, located approximately 4 cm above the apex of the heart, provided a more tractable geometry for the initial studies on the effects of adaptive control of errors and local regularization.

Adaptive Meshing

Test data for the adaptive algorithm consisted of a simulated dipolar source distribution placed on the surface of the heart model. Using the procedure described above, we computed direct solutions for different levels of mesh refinement and compared their effect on the potentials computed at the outer torso boundary. Figure 1 shows the voltage at the outer boundary versus distance around the two-dimensional contour for the original and five iterations of the adapted mesh. The original mesh contained approximately 1500 elements while the final mesh, after five iterations of the adaptive algorithm, contained approximately 7000 elements. The maximum estimated error in the calculated potential was over 30% greater in the original mesh compared to the final mesh and the maximum estimated error in the potential gradient was over 13% larger in the original mesh compared to the refined mesh. Increased accuracy does not come without a price; this h -adaptation increases the number of degrees of freedom, and thus, the computational costs. In our experience, however, this technique permits a fairly simple choice between accuracy and CPU expense because

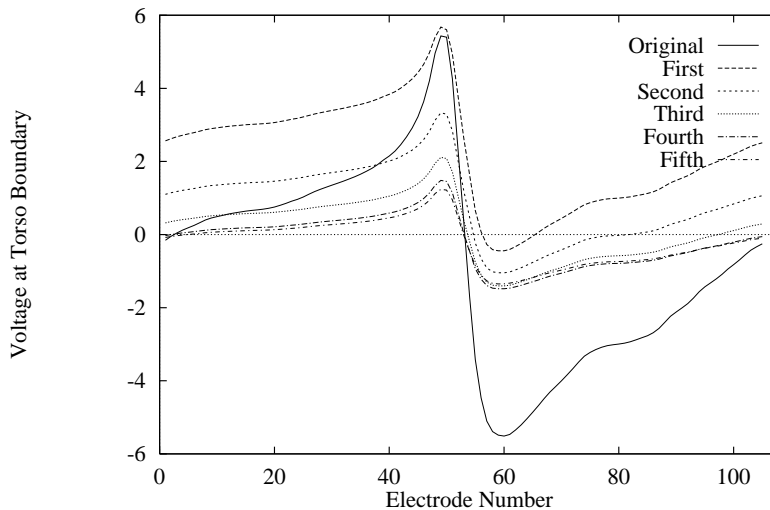


Figure 1: Effects of Automatic Mesh Refinement. The graphs shows potential value versus node number for the sequence of nodes around the outer perimeter of the two-dimensional geometry for a sequence of mesh refinements.

the relative error falls off rapidly with increasing degrees of freedom and then levels out after only a few iterations of the adaptive algorithm.

Local Regularization

To test the local regularization, we applied epicardial potentials recorded during open chest surgery from a cardiac arrhythmia patient as the Dirichlet boundary conditions of the two-dimensional model described above. The tissue conductivities were assigned as follows: fat = .045 S/m, epicardial fat-pad = .045 S/m, lungs = .096 S/m, skeletal muscle (in the fiber direction) = .3 S/m, skeletal muscle (across the fiber direction) = .1 S/m, and an average thorax value = .24 S/m. Forward solutions calculated using the adapted mesh served as torso boundary conditions, $\Phi = \Phi_0$ on $\Sigma \subseteq , T$ for the inverse solution both with and without 10% added Gaussian noise.

For the sub-matrices A_{VE} and A_{TV} , the *L-curve* algorithm determined the optimal *a priori* regularization parameter. The local Tikhonov regularization technique was then applied to the two sub-matrices and the inverse solution matrix computed. Because the size of the two-dimensional finite element model was relatively small, the calculations stayed in dynamic memory on an SGI

Indigo2 workstation and completed within a few seconds. To evaluate the results, we compare the locally regularized inverse solutions to those from a global Tikhonov regularization as well as the known epicardial solutions.

The application of the local regularization technique with the GSVD recovered the voltages to within 6.1% relative root-mean-squared (RMS) error of the true solution. This compares with a previous best from our work of 12.1% relative error⁴². Previous studies have reported the recovery of epicardial potentials with errors in the range of 20–100%,^{38, 43–46, 12, 11}, although in these cases investigators used three-dimensional geometric models and in some cases measured potentials on both epicardial and torso surfaces. We used another common strategy^{12, 11, 14} of applying a forward solution to measured epicardial potentials in order to generate the torso potentials, which, with added noise, served as the input to the inverse procedure. Figure 2 shows the inverse solution calculated using the local regularization technique compared with the recorded heart voltages as a function of position on the epicardium. The global solution tended to be smoother, not able to follow the extrema as well as the local solution could. The local regularized solution also showed a few areas of local error which suggest that a different partitioning of the sub-matrices might provide even better accuracy. In Figures 3 we show the errors between global and local regularizations and the exact potentials.

One of the interesting effects of the GSVD-based local regularization method is its stability when random noise is added to the thorax potentials. The GSVD-based local method is affected very little by the addition of 10% Gaussian noise in sharp contrast to the effects of noise on the Tikhonov solution as shown in Figures 4 and 5 .

There have been other approaches to local regularization reported in the literature recently. Approaches that are local in time, *i.e.*, that vary the regularization parameter as a function of time step, were proposed by Iakovidis and Gulrajani⁴⁷. Oster and Rudy have proposed a method they have named “regional regularization”, in which they decomposed the body surface potential maps—the input data to the electrocardiographic inverse problem—using either Legendre polynomials or singular value decompositions for concentric and eccentric spherical geometric models

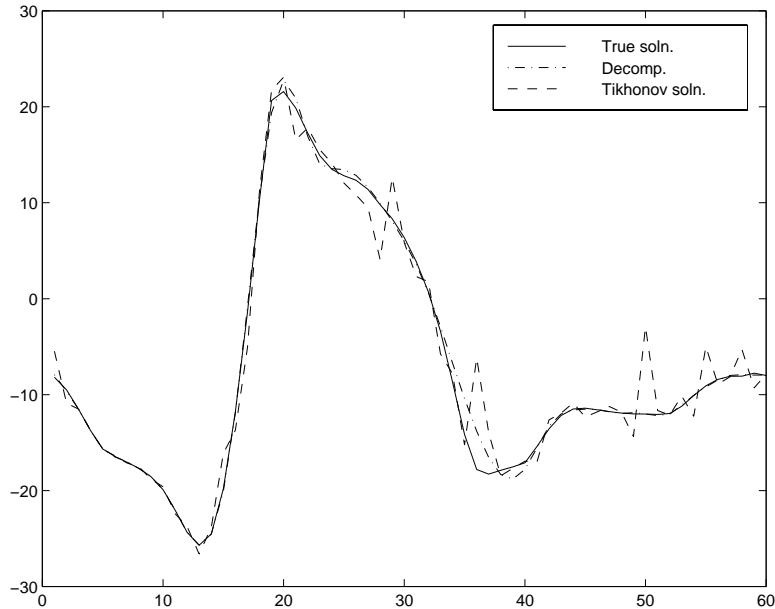


Figure 2: Local GSVD-based regularization technique. The figure shows the GSVD local regularization solution (marked Decomp), the best Tikhonov solution, and true solution.

for which analytic solutions exist¹¹. They then applied individual regularization to components of the decomposition, producing improvements in the accuracy of the resulting inverse solution. This regional regularization technique differs from that presented here in that the link between components of the decomposition and actual regions of the geometry is only indirect—the decomposition is based on signal content and not geometry. This feature is also a strength of the regional approach in that regularization changes with the input data and their signal-to-noise ratio.

A fundamentally different approach to solving the inverse problem that also permits local weighting is that proposed by Brooks *et al.*^{48,12}. Termed the “admissible solution approach”, this solution strategy does not include regularization but instead seeks to restrict the allowable solution space iteratively based on a wide variety of constraints, all applied simultaneously. In order to apply such constraints locally, a matrix based on the forward solution matrix (and hence the problem geometry) determines the weighting of each constraint on each node in the geometric model. The form of the weighting matrix can be freely selected to reflect *a priori* knowledge of the problem or made to depend on the input data. In one example, Brooks *et al.* varied the local weighting of constraints

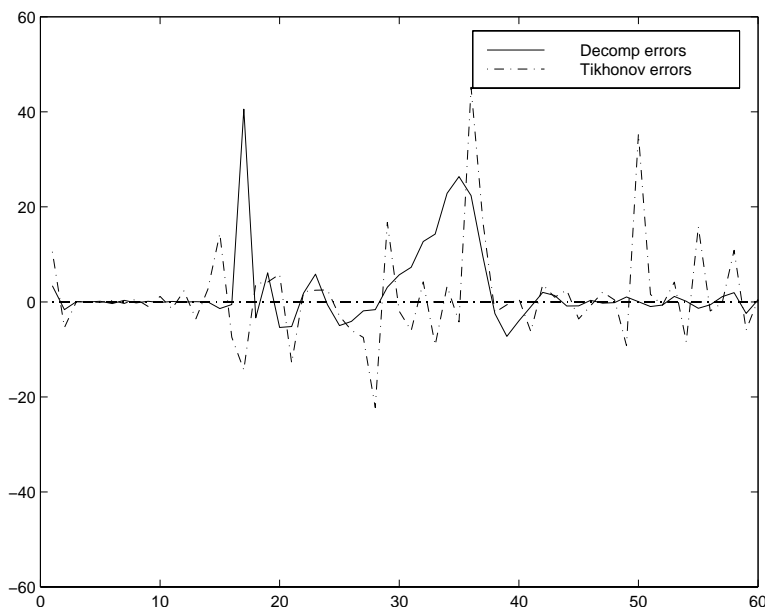


Figure 3: Errors for local and global regularization techniques. The figure shows the errors for the local solution (marked Decomp) and global Tikhonov for the solutions in the previous figures as functions of node number.

based on an estimate of the Laplacian from the (known) epicardial distributions, emphasizing the constraints in regions of small Laplacian and deemphasizing them in regions of larger Laplacian. One result was an improvement in the reconstruction of epicardial potential amplitudes. While this weighting approach is very similar to that applied here in that it is explicitly attached to the problem geometry, the admissible solutions method is fundamentally different from the Tikhonov regularization that we have used.

Implementation of Inverse Solutions

While great progress has been made in the modeling and simulation of bioelectric inverse problems over the last several years, there remain obstacles to the use of the modeling and simulation in the clinic. A particular hurdle lies in the complexity and inefficiency frequently encountered in the process of performing computational modeling. For example, the typical algorithm for performing electrocardiographic inverse simulations is as follows:

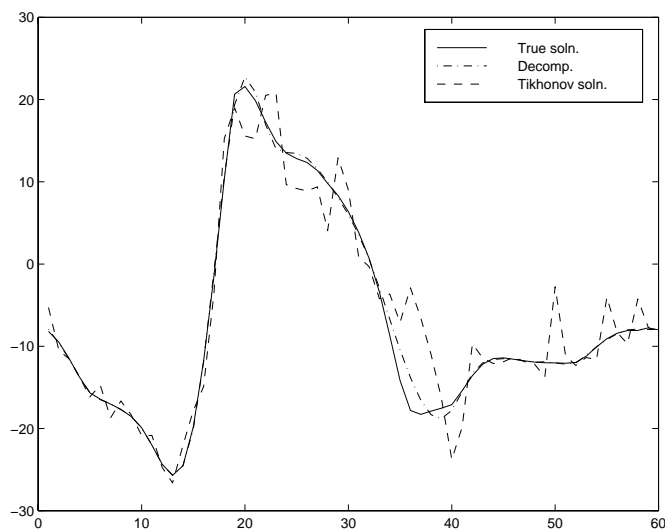


Figure 4: Effects of Noise on the GSVD and Tikhonov Solutions. Here 10% random noise has been added to torso potentials and the GSVD-based local regularization (Decomp) and Tikhonov solutions recomputed.

1. Create and/or modify a discretized geometric model.
2. Create and/or modify initial conditions and/or boundary conditions.
3. Compute numerical approximations to the generalized Laplace (or Poisson) equation, storing results on disk.
4. Apply regularization methods and perform error analysis.
5. Visualize and/or analyze results using a separate visualization program.
6. Make appropriate changes to the model.
7. Go back to step 1, 2, 3 and/or 4.
8. Repeat.

Changes to the model, input parameters, or computational processes are typically made using rudimentary tools, the most common being text editors. While the experienced scientist will incorporate some degree of automation into the process, usually via scripts, it remains time consuming and inefficient.

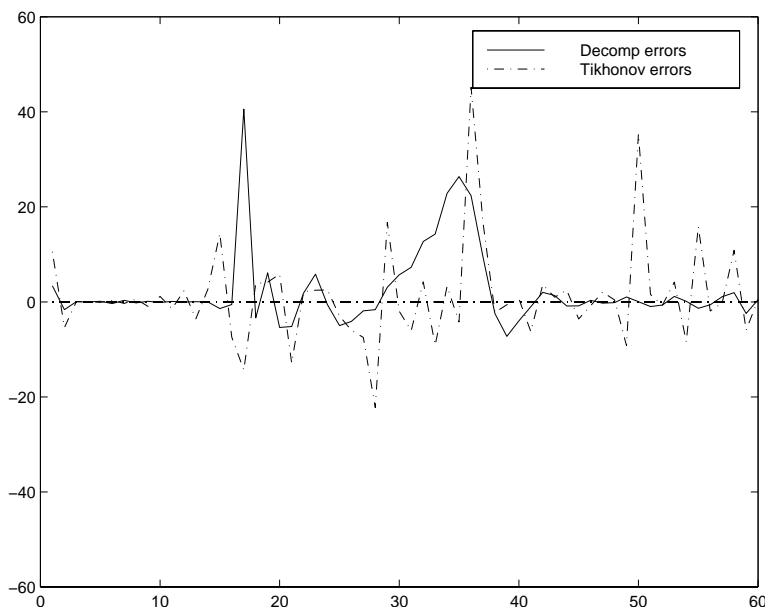


Figure 5: Errors for local and global regularization techniques with 10% added Gaussian noise. The figure shows the error as a function of node number after local (Decomp) and global Tokhonov regulatization.

To expedite the modeling, simulation, and visualization of computational inverse problems, we have developed a problem solving environment called SCIRun^{49–52}. SCIRun supports the interactive construction, debugging and steering of large-scale scientific computations through a “computational workbench,” implemented as a dataflow programming model. Key components of SCIRun include the ability to design, visualize, and modify geometric models, interactively change parameters and boundary conditions, adjust mesh discretization, and monitor both errors and system performance. Instead of the typical “off-line” simulation mode in which discrete programs perform each step of the computation, SCIRun “closes the loop” and allows interactive steering of all phases of the simulation. To permit the use of the dataflow programming paradigm even for large scientific problems, we have identified ways to avoid the excessive memory use inherent in standard dataflow implementations and have also implemented fine-grained dataflow in order to further promote computational efficiency. A sample SCIRun network to model the electrocardiographic forward/inverse problem is shown in Figure .

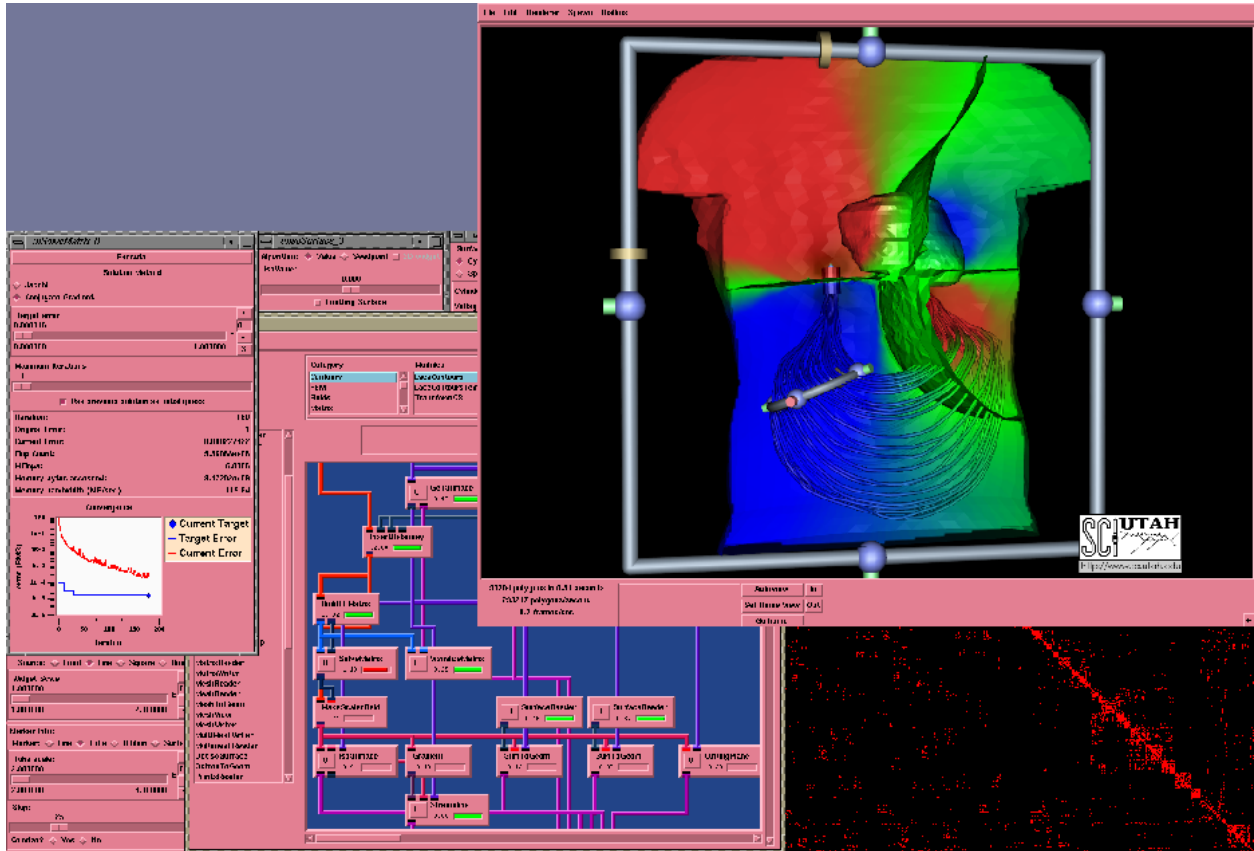


Figure 6: A sample SCIRun network showing the dataflow programming interface, user interfaces for controlling simulation parameters, and results from an large-scale electrocardiographic forward problem

Conclusion

We have described several new strategies—adaptive methods, generalized SVD local regularization techniques, and admissible solution approaches—to more accurately recover epicardial potentials from measured body surface potentials using an electrocardiographic inverse solution and discrete geometric models based on MRI. Furthermore, we have briefly presented a problem solving environment, SCIRun, for developing and testing new inverse algorithms, and visualizing model and solution results. Historically, two major challenges, one of obtaining enough accuracy in the inverse solution (a generally held opinion dictates that solution accuracy less than 10% RMS error is necessary for clinical application) and the ability to compute inverse solutions in a time-efficient manner, have impeded clinical utility of the electrocardiographic inverse solution. Recent develop-

ments of novel regularization methods like those described here suggest that major breakthroughs in numerical accuracy are within our reach. Integrated implementation environments like SCIRun provide a powerful set of tools for quickly transferring numerical solution ideas into a framework that permits rapid testing, tuning, and practical application. This combination will, we believe, soon lead to practical inverse solutions in medicine.

We are now pursuing the application of these methods to detailed, large-scale MRI-based thorax models, as well as head/brain models for electroencephalographic inverse problems.

Acknowledgments

This research was supported in part by awards from the NSF, the Nora Eccles Treadwell Foundation, and the Richard A. and Nora Eccles Harrison Fund for Cardiovascular Research.

References

- [1] R.M. Gulrajani, P. Savard, and F.A. Roberge. The inverse problem in electrocardiography: Solutions in terms of equivalent sources. *Crit. Rev. Biomed. Eng.*, 16:171–214, 1988.
- [2] Y. Yamashita. Theoretical studies on the inverse problem in electrocardiography and the uniqueness of the solution. *IEEE Trans Biomed. Eng.*, BME-29:719–725, 1982.
- [3] J.J.M. Cuppen. Calculating the isochrones of ventricular depolarization. *SIAM J. Sci. Statist. Comp.*, 5:105–120, 1984.
- [4] G.J. Huiskamp and A. van Oosterom. The depolarization sequence of the human heart surface computed from measured body surface potentials. *IEEE Trans Biomed. Eng.*, BME-35:1047–1059, 1989.
- [5] G.J. Huiskamp and A. van Oosterom. Tailored versus geometry in the inverse problem of electrocardiography. *IEEE Trans Biomed. Eng.*, BME-36:827–835, 1989.
- [6] Y. Rudy and B.J. Messinger-Rapport. The inverse solution in electrocardiography: Solutions in terms of epicardial potentials. *Crit. Rev. Biomed. Eng.*, 16:215–268, 1988.
- [7] R.M. Gulrajani, F.A. Roberge, and G.E. Mailloux. The forward problem of electrocardiography. In P.W. Macfarlane and T.D. Veitch Lawrie, editors, *Comprehensive Electrocardiology*, pages 197–236. Pergamon Press, Oxford, England, 1989.
- [8] R.M. Gulrajani, F.A. Roberge, and P. Savard. The inverse problem of electrocardiography. In P.W. Macfarlane and T.D. Veitch Lawrie, editors, *Comprehensive Electrocardiology*, pages 237–288. Pergamon Press, Oxford, England, 1989.
- [9] I. Iakovidis and C.F. Martin. A model study of instability of the inverse problem of electrocardiography. *Mathematical Biosciences*, 107:127–148, 1991.

- [10] C.R. Johnson and R.S. MacLeod. Local regularization and adaptive methods for the inverse Laplace problem. In D.N. Ghista, editor, *Biomedical and Life Physics*, pages 224–234. Vieweg-Verlag, Braunschweig, 1996.
- [11] H.S. Oster and Y. Rudy. Regional regularization of the electrocardiographic inverse problem: A model study using spherical geometry. *IEEE Trans Biomed. Eng.*, 44(2):188–199, 1997.
- [12] G.F. Ahmad, D. H Brooks, and R.S. MacLeod. An admissible solution approach to inverse electrocardiography. *Annal. Biomed. Eng.*, (in press):–, 1998.
- [13] D.H. Brooks, G. Ahmad, and R.S. MacLeod. Multiply constrained inverse electrocardiology: Combining temporal, multiple spatial, and and iterative regularization. In *Proceedings of the IEEE Engineering in Medicine and Biology Society 16th Annual International Conference*, pages 137–138. IEEE Computer Society, 1994.
- [14] D.H. Brooks, G.F. Ahmad, R.S. MacLeod, and G.M. Maratos. Inverse electrocardiology by simultaneous imposition of multiple constraints. *IEEE Trans Biomed. Eng.*, (in revision), 1998.
- [15] P.C. Hansen. Analysis of discrete ill-posed problems by means of the L-curve. *SIAM Review*, 34(4):561–580, 1992.
- [16] P.C. Hansen. *Rank-Deficient and Discrete Ill-Posed Problems: Numerical aspects of linear inversion*. PhD thesis, Technical University of Denmark, 1996.
- [17] R.S. MacLeod and D.H. Brooks. Recent progress in inverse problems in electrocardiology. *IEEE Eng. in Med. & Biol. Soc. Magazine*, (in press), January 1998.
- [18] R.S. MacLeod, R.M. Miller, M.J. Gardner, and B.M. Horáček. Application of an electrocardiographic inverse solution to localize myocardial ischemia during percutaneous transluminal coronary angioplasty. *J. Cardiovasc. Electrophysiol.*, 6:2–18, 1995.

- [19] H.S. Oster, B. Taccardi, R.L. Lux, P.R. Ershler, and Y. Rudy. Noninvasive electrocardiographic imaging: Reconstruction of epicardial potentials, electrograms, and isochrones and localization of single and multiple electrocardiac events. *Circ.*, 96(3):1012–1024, 1997.
- [20] C.J. Penney, J.C. Clements, M.J. Gardner, L. Sterns, and B.M. Horacek. The inverse problem of electrocardiography: application to localization of Wolff-Parkinson-White pre-excitation sites. In *Proceedings of the IEEE Engineering in Medicine and Biology Society 17th Annual International Conference*, pages 215–216. IEEE Press, 1995.
- [21] D.S. Burnett. *Finite Element Method*. Addison Wesley, Reading, Mass., 1988.
- [22] C. Johnson. *Numerical solution of Partial Differential Equations by the Finite Element Method*. Cambridge University Press, Cambridge, 1990.
- [23] G. Strang and G. Fix. *An Analysis of the Finite Element Method*. Prentice–Hall, Englewood Cliffs, NJ, 1973.
- [24] B. Szabó and I. Babuška. *Finite Element Analysis*. John Wiley & Sons, New York, 1991.
- [25] C.R. Johnson and R.S. MacLeod. Nonuniform spatial mesh adaption using a posteriori error estimates: applications to forward and inverse problems. *Applied Numerical Mathematics*, 14:311–326, 1994.
- [26] J.A. Schmidt, C.R. Johnson, J.C. Eason, and R.S. MacLeod. Applications of automatic mesh generation and adaptive methods in computational medicine. In I. Babuska, J.E. Flaherty, W.D. Henshaw, J.E. Hopcroft, J.E. Oliger, and T. Tezduyar, editors, *Modeling, Mesh Generation, and Adaptive Methods for Partial Differential Equations*, pages 367–390. Springer-Verlag, 1995.
- [27] P.G. Ciarlet and J.L. Lions. *Handbook of Numerical Analysis: Finite Element Methods*, volume 1. North-Holland, Amsterdam, 1991.

- [28] R. Rannacher and R. Scott. Some optimal error estimates for piecewise linear finite element approximations. *Math. Comp.*, 38:437–445, 1982.
- [29] J.E. Flaherty. *Adaptive Methods for Partial Differential Equations*. SIAM, Philadelphia, 1989.
- [30] O.C. Zienkiewicz and J.Z. Zhu. A simple error estimate and adaptive procedure for practical engineering analysis. *Int. J. Num. Meth. Eng.*, 24:337–357, 1987.
- [31] O.C. Zienkiewicz and J.Z. Zhu. Adaptivity and mesh generation. *Int. J. Num. Meth. Eng.*, 32:783–810, 1991.
- [32] I. Babuška. Error bounds for the finite element method. *Numer. Math.*, 16:322–333, 1971.
- [33] V.A. Morozov. *Methods for Solving Incorrectly Posed Problems*. Springer-Verlag, New York, 1984.
- [34] R. Kress. *Linear Integral Equations*. Springer-Verlag, New York, 1989.
- [35] G.H. Golub, M.T. Heath, and G. Wahba. Generalized cross-validation as a method for choosing a good ridge parameter. *Technometrics*, 21:215–223, 1979.
- [36] P.C. Hansen. Analysis of discrete ill-posed problems by means of the L-curve. *SIAM Review*, 34(4):561–580, 1992.
- [37] C.L. Lawson and R.J. Hanson. *Solving Least Squares Problems*. Prentice-Hall, Englewood Cliffs, NJ, 1974.
- [38] R.D. Throne, L.G. Olson, T.J. Hrabik, and J.R. Windle. Generalized eigensystem techniques for the inverse problem of electrocardiography applied to a realistic heart-torso geometry. *IEEE Trans Biomed. Eng.*, 44(6):447, 1997.
- [39] C.R. Johnson, R.S. MacLeod, and P.R. Ershler. A computer model for the study of electrical current flow in the human thorax. *Computers in Biology and Medicine*, 22(3):305–323, 1992.

- [40] C.R. Johnson, R.S. MacLeod, and M.A. Matheson. Computer simulations reveal complexity of electrical activity in the human thorax. *Comp. in Physics*, 6(3):230–237, May/June 1992.
- [41] K.R. Foster and H.P. Schwan. Dielectric properties of tissues and biological materials: A critical review. *Critical Reviews in Biomed. Eng.*, 17:25–104, 1989.
- [42] C.R. Johnson and R.S. MacLeod. Inverse solutions for electric and potential field imaging. In R.L. Barbour and M.J. Carvlin, editors, *Physiological Imaging, Spectroscopy, and Early Detection Diagnostic Methods*, volume 1887, pages 130–139. SPIE, 1993.
- [43] P. Colli Franzone, G. Gassaniga, L. Guerri, B. Taccardi, and C. Viganotti. Accuracy evaluation in direct and inverse electrocardiology. In P.W. Macfarlane, editor, *Progress in Electrocardiography*, pages 83–87. Pitman Medical, 1979.
- [44] P. Colli Franzone, L. Guerri, S. Tentonia, C. Viganotti, S. Spaggiari, and B. Taccardi. A numerical procedure for solving the inverse problem of electrocardiography. Analysis of the time-space accuracy from *in vitro* experimental data. *Math. Biosci.*, 77:353, 1985.
- [45] B.J. Messinger-Rapport and Y. Rudy. Regularization of the inverse problem in electrocardiography: A model study. *Math. Biosci.*, 89:79–118, 1988.
- [46] P.C. Stanley, T.C. Pilkington, and M.N. Morrow. The effects of thoracic inhomogeneities on the relationship between epicardial and torso potentials. *IEEE Trans Biomed. Eng.*, BME-33:273–284, 1986.
- [47] I. Iakovidis and R.M. Gulrajani. Regularization of the inverse epicardial solution using linearly constrained optimization. In *Proceedings of the IEEE Engineering in Medicine and Biology Society 13th Annual International Conference*, pages 698–699. IEEE Press, 1991.
- [48] G.F. Ahmad, D.H. Brooks, C.A. Jacobson, and R.S. MacLeod. Constraint evaluation in inverse electrocardiography using convex optimization. In *Proceedings of the IEEE Engineering in*

- Medicine and Biology Society 17th Annual International Conference*, pages 209–210. IEEE Press, 1995.
- [49] S.G. Parker, D.M. Weinstein, and C.R. Johnson. The SCIRun computational steering software system. In E. Arge, A.M. Bruaset, and H.P. Langtangen, editors, *Modern Software Tools in Scientific Computing*, pages 1–44. Birkhauser Press, 1997.
- [50] C.R. Johnson and S.G. Parker. A computational steering model for problems in medicine. In *Supercomputing '94*, pages 540–549. IEEE Press, 1994.
- [51] C.R. Johnson and S.G. Parker. Applications in computational medicine using SCIRun: A computational steering programming environment. In *Supercomputer '95*, pages 2–19. Springer-Verlag, 1995.
- [52] S.G. Parker and C.R. Johnson. SCIRun: A scientific programming environment for computational steering. In *Supercomputing '95*. IEEE Press, 1995.